pressure and exhaust pressure at the end of the stroke as temperature increases.

For space power cycles, a more important parameter than thermal efficiency is system weight. Since the major part of the system is radiator weight, turbine and piston were compared with regard to a radiator weight factor, $(1 - \eta)/\eta T_c^4$, which is normalized to a given design. It represents the area, and hence weight, needed to reject the waste heat from the cycle. Figure 4 shows the effect of varying condenser temperature on this factor for a fixed boiler temperature of 2400°F. There is a minimum in the curve because $\eta \to 0$ as $T_c \to T_B$ and $T_c^4 \to 0$ as $T_c \to 0$. The minimum weight for the turbine expansion corresponds to a piston expansion of $V_F/V_0 = 5/1$. However, a piston expansion of V_F/V_0 of 2/1 adds only 15% more weight, because the lower efficiency is offset by a higher condenser temperature.

Figure 5 shows the locus of all the minimum radiator weights for different expansions and boiler temperatures. Again note that a piston expansion of 2/1 closely approaches a turbine expansion. A 2/1 expansion MHD generator would weigh about 0.65 lb/kw(e) as compared to 0.5 lb/kw(e) for the constant pressure generator.

Thus, piston devices of low expansion ratios, e.g., 2/1, can approach, within a few percent, thermal efficiencies and system weights of turbines for Rankine alkali metal space power cycles.

References

[1] Powell, J., "Summary of direct conversion work at BNL," Brookhaven National Lab. Rept. BNL 8199 (1964).

[2] Deem, H. W., "The specific heat from 0 to 1150°C and the heat of fusion of potassium," Battelle Memorial Inst. BATT-4673-T2 (1962).

[3] Grosse, A. V., "High temperature research," Science **140**, 781–789 (1963).

[4] Walling, J. F., "The vapor pressure and heat of vaporization of potassium from 480 to 1150°C," Battelle Memorial Inst. BATT 4673-T3 (1963).

[5] Lemmon, A., private communication (1964).

A Simple Approach to the Multicomponent Laminar Boundary Layer

A. Casaccio* and S. Cousin†

Republic Aviation Corporation, Farmingdale, N. Y.

Owing to the difficulties usually encountered in numerical solutions of the boundary-layer equations, there exists a necessity for approximate methods by which one may obtain over-all boundary-layer characteristics. One of the more prominent approaches to this problem is to consider that the flow is locally similar. The validity of the approach relies on the condition that the properties of the fluid at the external and body-surface boundaries are slowly varying functions of the streamwise coordinate.

The method presented herein is based on this local similarity premise as applied to the multicomponent laminar boundary layer with either frozen or equilibrium chemistry prevailing. Accordingly, it is possible to transform the governing conservation equations to the form

$$(Cf'')' + ff'' = (2\xi/u_e)(du_e/d\xi)[f'^2 - (\rho_e/\rho)] \quad (1)$$

$$(Cg')' + fg' = 0 \quad (2)$$

$$(Cz_i')' + fz_i = 0 \quad (3)$$

by utilizing the Levy-Lees transformation

$$\xi = \int_0^s \rho_*\mu_* u_e r^{2j} ds \qquad \eta = \frac{\rho_e u_e r^j}{(2\xi)^{1/2}} \int_0^y \frac{\rho}{\rho_e}\, dy$$

and considering unit values of the Prandtl and Lewis numbers and Υ_{ie} equal to a constant.

In order to obtain a solution for the system [Eqs. (1–3)], it is necessary to specify the coupling existing between the density and enthalpy. If, in accordance with the approach of Ref. 1, a new parameter $\phi(\eta)$ is introduced, defined by

$$\phi(\eta) = (g - \lambda)/(1 - \lambda) \quad (4)$$

and an empirical relation of the form

$$\rho_e/\rho = (1 - \kappa)f'^2 + \kappa\phi \quad (5)$$

is adopted, there results for Eqs. (1–3)

$$f''' + ff'' = \beta(f'^2 - \phi) \quad (6)$$

$$\phi'' + f\phi' = 0 \quad (7)$$

$$z_i'' + fz_i' = 0 \quad (8)$$

subject to conditions

$$f(0) = f'(0) = 0 \qquad \phi(0) = \phi_w \qquad z_i(0) = z_{iw} \quad (9)$$

$$f', \phi, z_i \to 1 \qquad f'', \phi', z_i' \to 0 \quad \text{as } \eta \to \infty \quad (10)$$

when it is assumed that $C = \rho\mu/\rho_*\mu_* = 1$ and $\beta = (2\kappa\xi/u_e) \times (du_e/d\xi)$ is a constant. It is evident from Eqs. (7) and (8) that a Crocco-type relation exists between $\phi(\eta)$ and $z_i(\eta)$, i.e.,

$$z_i = [1/(1 - \phi_w)][(z_{iw} - \phi_w) + (1 - z_{iw})\phi] \quad (11)$$

and that the solutions to Eqs. (6) and (7) subject to boundary conditions (9) and (10) are those given by Cohen and Reshotko.[2] The constants λ and κ of Eqs. (4) and (5) are to be determined by insuring the satisfaction of Eq. (5) at as many points in the boundary layer as possible.

Fitting the Density Ratio

Since Eq. (5) is identically satisfied at the outer edge of the layer, λ and κ can be evaluated by matching the density and its derivative at the body surface. Hence, there results[1]

$$\lambda = (h_w/H_e) - (c_{pw}/\alpha_w H_e) \quad (12)$$

$$\kappa = (\rho_e/\rho_w)[1 + (\alpha_w/c_{pw})(H_e - h_w)] \quad (13)$$

where

$$c_p = \left(\frac{\partial h}{\partial T}\right)_p \qquad \alpha = \rho\left(\frac{\partial(1/\rho)}{\partial T}\right)_p = \frac{1}{T}\left[1 - \frac{T}{W}\left(\frac{\partial W}{\partial T}\right)_p\right] \quad (14)$$

Consistent with the local similarity assumption, λ, κ, and β, which are in general functions of streamwise location, are considered locally to be specific constants varying from each locally similar section to the next. The history of the downstream flow is retained only in the ξ dependence of the similarity parameter η. Furthermore, heat-transfer correlations have indicated that the reference conditions should be based on the local reference enthalpy value, which is compatible with the local similarity approach.

Specification of the Physical Pressure Gradient

Using the momentum equation at the outer edge and the transformation conditions, it is possible to express β according to

$$\beta = -2\kappa \frac{dp}{ds} \frac{\int_0^s \rho_*\mu_* u_e r^{2j} ds}{\rho_e u_e^3 \rho_*\mu_* r^{2j}} \quad (15)$$

Received October 28, 1964. This work was performed under U. S. Air Force Contract No. AF33(657)-9697 Air Force Flight Dynamics Laboratory, Research and Technology Division.

* Head, Heat Transfer and Combustion Group, Hypersonic Vehicles. Member AIAA.

† Principle Research and Development Engineer, Hypersonic Vehicles.

For the equilibrium flow case, the thermodynamic and transport properties involved in Eq. (15) can be evaluated according to the air model suggested in Ref. 3. Thus

$$\rho_*\mu_* = \frac{0.225\rho_r\mu_r}{1.0213(h_*/h_E)^{0.3329} - 0.0213}\left(\frac{p}{p_r}\right)^{0.992} \quad (16)$$

where

$$\frac{h_*}{h_E} = \frac{1}{2}\left[\frac{h_w}{h_E} + \frac{H_e}{h_E}\left(1 - \frac{u_e^2}{2H_e}\right)\right] + 0.22(P_{r*})^{1/2}\frac{H_e}{h_E}\frac{u_e^2}{2H_e} \quad (17)$$

and where the quantities ρ_r, μ_r, p_r, and h_E are constants.[3] Furthermore, by considering local hypersonic flow ($u_e^2 \approx 2H_e$), constant wall enthalpy (thus $h_* = \text{const}$), and a pressure variation in the physical plane governed by $p \sim \bar{s}^n$ where

$$\bar{s} = \int_0^s r^{2j}ds$$

it is possible to show that

$$\beta = -\frac{\kappa p}{\rho_e H_e}\left(\frac{n}{0.992n + 1}\right) = -(1 - \lambda)\frac{p}{\rho_w}\frac{\alpha_w}{c_{pw}}\left(\frac{n}{0.992n + 1}\right) \quad (18)$$

Using the relationships given in Ref. 3, there results for α_w/c_{p_w} the relation

$$\frac{\alpha_w}{c_{p_w}} = \frac{0.6415(h_w/h_E)^{-0.3877}}{h_E[1.0477(h_w/h_E)^{0.6123} - 0.0477]} \quad (19)$$

which implies that (α_w/c_{p_w}) is a constant since (h_w/h_E) is constant. In addition, for wall temperatures of practical interest (cold wall), the mole fractions of the dissociated air species at the wall are virtually independent of pressure in the range ($0.001 \leq p \leq 10$ atm). Accordingly, the molecular weight at the wall is a constant as are the species enthalpies, temperature, and pressure-density ratio. As a result

$$\beta = -(1 - \lambda)\frac{\alpha_w}{c_{pw}}\frac{RT_w}{W_w}\left(\frac{n}{0.992n + 1}\right) = \text{const} \quad (20)$$

for specific values of n. For the temperature and pressure range mentioned previously, $(T_w/W_w)(\partial W/\partial T)_{p,w} \approx 0$, thereby reducing the general expression for the coefficient of thermal expansion at the wall to $\alpha_w \approx 1/T_w$. Consequently, Eq. (20) becomes

$$\beta = -(1 - \lambda)(R/W_w c_{pw})[n/(0.992n + 1)] \quad (21)$$

or

$$\beta = -(1 - \lambda)[(\gamma_{ew} - 1)/\gamma_{ew}][n/(0.992n + 1)] \quad (22)$$

if γ_{ew} is defined as

$$\gamma_{ew} = c_{pw}/[c_{pw} - (R/W_w)] \quad (23)$$

Since $\lambda = 0$ and $\gamma_{ew} = \gamma = 1.4$, for an ideal single component gas, it is seen from Eq. (22) that β reduces almost exactly to the well-known perfect gas relationship. The factor 0.992 appears instead of unity because the expression used for $\rho\mu$ does not reduce exactly to its ideal gas counterpart.

For the frozen flow case, the evaluation of β differs since the species concentrations are no longer unique functions of pressure and temperature but must be evaluated in accordance with Eq. (11). In general, from kinetic theory

$$\rho\mu = \frac{266.93 \times 10^{-7}}{Ak^a}\frac{pW}{R}T^{-[(1/2)+a]}\times \sum_i\left[W_i^{1/2}\epsilon_i^a\Upsilon_i/\sigma_i^2\left(\Upsilon_i + \sum_{k\neq i}G_{ik}\Upsilon_k\right)\right] \quad (24)$$

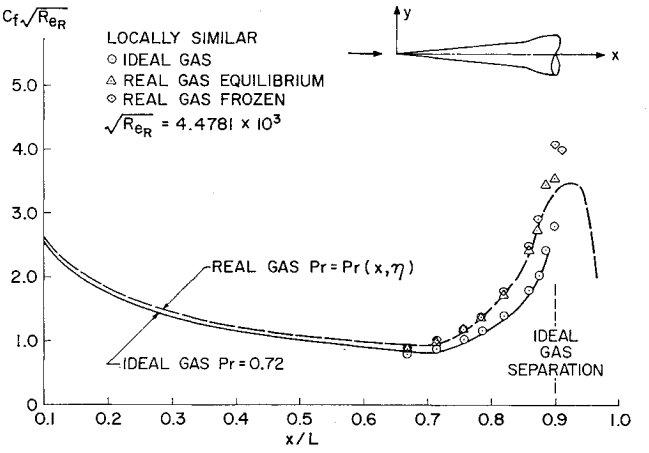

Fig. 1 Laminar skin-friction coefficient vs x/L on 50-ft flight vehicle at Mach = 20 and 154,000 ft.

where ϵ_i is the depth of the potential well in the Lennard-Jones potential, k is Boltzmann's constant, σ_i is the collision diameter, Υ_i are the species mass fractions, and

$$G_{ik} = \frac{[1 + (\sigma_k/\sigma_i)(\epsilon_i/\epsilon_k)^{a/2}]^2(W_i/W_k)}{(2)^{3/2}[1 + (W_i/W_k)]^{1/2}}$$

The reduced collision integral $\bar{\Omega}^{(2,2)}$, with the use of the Lennard-Jones interparticle potential function, has been replaced by $\bar{\Omega}^{(2,2)} = A\bar{T}_i^a$ where it was found that, for the range ($1.0 \leq \bar{T}_i = kT/\epsilon_i \leq 400$), a very good representation of this integral is obtained by using $A = 1.153$ and $a = -0.1459$. From the general relationship given by Eq. (24) it is evident that functionally $\rho_*\mu_* = \rho\mu(p, T_*, \Upsilon_{i*})$.

If the frozen composition is composed of s species of which e are the basic undissociated constituents, then the atom concentrations across the boundary layer are given by

$$z_i = \Upsilon_i/\Upsilon_{ie} = (g - g_w)/(1 - g_w) \qquad g = H/H_e \qquad (i = 1, 2, \ldots, s - e) \quad (25)$$

for the catalytic wall case, and $\Upsilon_i = \Upsilon_{ie}$ ($i = 1, 2, \ldots, s - e$) for the noncatalytic wall case. By relating Eq. (17) to the enthalpy-velocity relation at the reference state it can be shown that

$$g_* = \tfrac{1}{2}(1 - g_w) \quad (26)$$

As a result, the reference concentrations become

$$\Upsilon_{i*} = (\Upsilon_{ie} + \Upsilon_{iw})/2 \qquad (i = 1, 2, \ldots, e)$$

$$\Upsilon_{i*} = \Upsilon_{ie}/2 \qquad (i = 1, 2, \ldots, s - e) \quad (27)$$

for the catalytic wall and $\Upsilon_{i*} = \Upsilon_{ie}$ ($i = 1, 2, \ldots, s$) for the noncatalytic wall.

Since it has been shown already that Υ_{iw}, Υ_{ie}, and h_* are constants, it follows that Υ_{i*} and T_* are also constants. Accordingly, $\rho_*\mu_*$ becomes expressible as $\rho_*\mu_* = K_{i*}p$, where

$$K_{i*} = \frac{266.93 \times 10^{-7}}{Ak^a}\frac{W_*}{R}T_*^{-(1/2+a)}\times \sum_i\left[W_i^{1/2}\epsilon_i^a\Upsilon_{i*}/\sigma_i^2\left(\Upsilon_{i*} + \sum_{k\neq i}G_{ik}\Upsilon_{k*}\right)\right] \quad (28)$$

is constant for each species. With this result it is possible to show that

$$\beta = -(1 - \lambda_f)\frac{R}{W_w c_{pw}}\left(\frac{n}{n + 1}\right) = -(1 - \lambda_f)\times \left(\frac{\gamma_f - 1}{\gamma_f}\right)\left(\frac{n}{n + 1}\right) \quad (29)$$

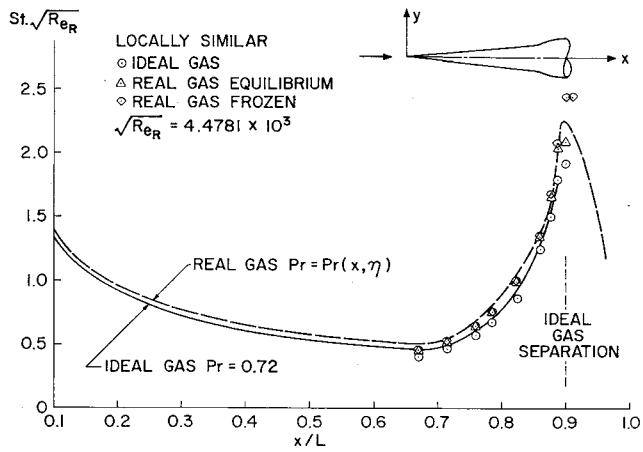

Fig. 2 Laminar heat-transfer parameter vs x/L on 50-ft flight vehicle at Mach = 20 and 154,000 ft.

by following a similar procedure as outlined for the equilibrium flow case. In Eq. (29)

$$\lambda_f = (1/H_e)(h_w - c_{pw}T_w)$$

and

$$\gamma_f \left(\sum_i c_{pi}X_i - R \right) = \sum_i c_{pi}X_i$$

Numerical Example

In Figs. 1 and 2 heat-transfer and skin-friction results obtained by the present method are compared with those of the more exact numerical equilibrium flow procedure of Ref. 4. The calculation was performed for an axisymmetric sharp-nosed compression body characteristic of a supersonic ramjet inlet forebody for flight conditions corresponding to $M_\infty = 20$ at 154,000 ft and for a wall temperature of 2300°R. Although the local similarity concept is restricted to flows with slowly varying external properties, its accuracy for the body contour considered proved to be remarkably good despite the limitations imposed on the Prandtl and Lewis numbers and on the variation of $\rho\mu$. For the conditions considered, very little difference was observed between the frozen flow results, for both catalytic and noncatalytic surfaces, and those of the equilibrium case. The only appreciable difference noted between the two calculations occurs near the end of the compression surface where the dissociation level is highest. This is not surprising, since for slender shapes the dissociation level in the stream is quite low, thereby minimizing the difference between the frozen and equilibrium assumptions. A complete development of the present method, together with additional numerical results and comparisons, is available in Ref. 5.

References

[1] Hayes, W. D., "On laminar boundary layers with heat transfer," Jet Propulsion **26**, 270–274 (1956).

[2] Cohen, C. B. and Reshotko, E., "Similar solutions for the compressible laminar boundary layer with heat transfer and pressure gradient," NACA TR 1293 (1956).

[3] Cohen, N. B., "Correlation formulas and tables of density and some transport properties of equilibrium dissociating air for use in solutions of the boundary layer equations," NASA TN-D-194 (February 1960).

[4] Clutter, D. and Smith, A. M. O., "Solution of the general boundary layer equations for compressible laminar flow including transverse curvature," Douglas Aircraft Rept. LB 31088 (February 1963).

[5] Sanator, R. J., Savage, S. B., DeCarlo, J. P., Torrillo, D. T., Casaccio, A., and Cousin, S. B., "Experimental and theoretical investigation of inlets for supersonic combustion ramjets," U. S. Air Force Flight Dynamics Lab., Wright-Patterson Air Force Base, Tech. Doc. Rept. FDL TDR 64-119 (October 1964).

Hypersonic Boundary-Layer Transition Data for a Cold-Wall Slender Cone

R. J. Sanator,* J. P. DeCarlo,† and D. T. Torrillo‡
Republic Aviation Corporation, Farmingdale, N. Y.

Nomenclature

c_p = specific heat at constant pressure
M = Mach number
q = heat-transfer rate
r = nose or body radius
Re_∞ = Reynolds number per foot based on freestream conditions
Re_s = Reynolds number based on local properties and on distance along surface from stagnation point or tip = $\rho_e u_e s/\mu_e$
St = Stanton number = $q_w/\rho_e u_e c_p(T_{AW} - T_W)$
s = distance along surface from stagnation point or tip of body
T = absolute temperature
u = velocity component along the body
μ = coefficient of absolute viscosity
ρ = mass density

Subscripts

AW = adiabatic wall
B = body
e = local flow at edge of boundary layer
N = nose
t = transition
w = wall value
0 = stagnation value in freestream
∞ = freestream static values

Introduction

SOME recent experimental data are presented concerning the effect of wall-cooling, nose-bluntness, and roughness elements on the transition of the hypersonic boundary layer on a slender cone. This data constitutes an extension to higher Mach numbers of available information on boundary-layer transition recently compiled and presented in Ref. 1.

Nose blunting and wall cooling are known in some cases to alter significantly the location of transition, giving rise to the phenomenon of transition reversal. The location of transition has important ramifications in vehicle design, in that it affects the local heat-transfer rate to the body surface, the skin-friction drag, and the susceptibility of the boundary layer to separation. In the design of hypersonic inlets, both the state of the boundary layer and transition location have a significant influence on the inlet performance. The data presented here comprise part of the results obtained in the experimental investigation of hypersonic inlet performance reported on in Ref. 2.

Discussion

The model used in the investigation was a right-circular cone configuration having a semivertex angle of 5° and a

Received October 29, 1964. The research material reported in this paper was sponsored by the Flight Dynamics Laboratory, Research and Technology Division, Air Force Systems Command, U. S. Air Force under Contract No. AF33(657)-9697. This research program was conducted under the technical cognizance of G. Keith Richey of the Internal Aerodynamics Section of the Flight Dynamics Laboratory. The wind tunnel tests were conducted by S. N. Schmotolocha and T. Himka of the Hypersonic Wind Tunnel Staff of Republic Aviation Corporation.

* Assistant Manager, Hypersonic Vehicles, Aircraft Division. Associate Fellow Member AIAA.

† Principle Aerodynamics Engineer, Aircraft Division. Associate Member AIAA.

‡ Specialist Aerodynamics Engineer, Aircraft Division. Member AIAA.